COMPUTER VISION

Autonomous tracking of honey bee behaviors over long-term periods with cooperating robots

Jiří Ulrich[1]†, Martin Stefanec[2]†, Fatemeh Rekabi-Bana[3]†, Laurenz Alexander Fedotoff[2], Tomáš Rouček[1], Bilal Yağız Gündeğer[4], Mahmood Saadat[3], Jan Blaha[1], Jiří Janota[1], Daniel Nicolas Hofstadler[2], Kristina Žampachů[1], Erhan Ege Keyvan[5], Babür Erdem[5], Erol Şahin[4], Hande Alemdar[4], Ali Emre Turgut[6], Farshad Arvin[3], Thomas Schmickl[2]*‡, Tomáš Krajník[1]‡

Digital and mechatronic methods, paired with artificial intelligence and machine learning, are transformative technologies in behavioral science and biology. The central element of the most important pollinator species—honey bees—is the colony's queen. Because honey bee self-regulation is complex and studying queens in their natural colony context is difficult, the behavioral strategies of these organisms have not been widely studied. We created an autonomous robotic observation and behavioral analysis system aimed at continuous observation of the queen and her interactions with worker bees and comb cells, generating behavioral datasets of exceptional length and quality. Key behavioral metrics of the queen and her social embedding within the colony were gathered using our robotic system. Data were collected continuously for 24 hours a day over a period of 30 days, demonstrating our system's capability to extract key behavioral metrics at microscopic, mesoscopic, and macroscopic system levels. Additionally, interactions among the queen, worker bees, and brood were observed and quantified. Long-term continuous observations performed by the robot yielded large amounts of high-definition video data that are beyond the observation capabilities of humans or stationary cameras. Our robotic system can enable a deeper understanding of the innermost mechanisms of honey bees' swarm-intelligent self-regulation. Moreover, it offers the possibility to study other social insect colonies, biocoenoses, and ecosystems in an automated manner. Social insects are keystone species in all terrestrial ecosystems; thus, developing a better understanding of their behaviors will be invaluable for the protection and even the restoration of our fragile ecosystems globally.

INTRODUCTION

Amid an emerging ecological diversity crisis, our biosphere is facing unprecedented losses in species richness and biomass (*1*–*3*). Among the most decimated groups are insects (*4*, *5*), resulting in a severe pollination crisis (*6*). This harms not only our natural ecosystems but also our agricultural efforts in terms of crop production (*7*), which in turn can lead to economic inflation (*8*) and ultimately endanger the food security of our society (*9*).

Honey bees are the most important pollinator species, providing about 50% of pollination to pollinator-dependent crops (*10*). Because they are easy to breed commercially and can be centrally housed in a managed hive, they can potentially be used to compensate for the losses that we face across the thousands of other pollinator species (*11*). Their centralized way of living in large numbers as a "superorganism" means that complex self-regulation is required, and the process by which their collective decisions are made is often termed "swarm intelligence" (*12*). To date, we only understand a fraction of the mechanisms of their swarm intelligence; thus, a system that is capable of observing the behavior of honey bees can be a powerful tool to extensively study colony integration (*13*). The specific behaviors of the queen and the worker bees (Fig. 1, A and B) and comb-based activities are of interest, and they include, for instance, brood development (Fig. 1C) and other behaviors related to distributed self-organization and self-regulating feedback loops.

The pollination potential and the winter survival rates of honey bee colonies depend mainly on their population size and the health of the workers (*14*). Both winter survival and pollination potential can be studied in the brood nest, because all honey bees, and also all of their parasites, are (re)produced in this comb area (*15*). Ultimately, all worker bees hatch from the eggs laid by a single queen, a behavior known as oviposition behavior. Oviposition behavior is typically observed in the central brood nest area (*16*) and is the most important factor in colony growth and reproduction (*17*). Many crucial aspects of the self-organization of the superorganism depend on the interactions between the colony and the queen (*18*), mediated by the "queen court," a group of worker bees of a certain age that perform essential tasks for the queen, such as feeding or cleaning her (*19*). Typically, a honey bee queen spends 99.99% of her life inside her hive, with the only exceptions being a few mating flights at the beginning of her adult lifetime and occasional swarming events in colony-level reproduction. Thus, using a system to study the honey bee queen and her interactions with worker bees and comb cells is of the utmost importance for developing a fundamental understanding of the core mechanisms of the honey bee colony (Fig. 1). Behavioral observation is particularly meaningful if the organisms being studied are observed in their natural context. Thus, systems that allow observations of queens within a fully functioning beehive are expected to yield better insights and fewer behavioral artifacts compared with controlled laboratory experiments. However, multifactorial models and noise interpretation are required for such hive-based observations.

[1]Artificial Intelligence Centre, Faculty of Electrical Engineering, Czech Technical University, Prague, Czechia. [2]Artificial Life Lab, Department of Zoology, Institute of Biology, University of Graz, Graz, Austria. [3]Swarm & Computation Intelligence Lab (SwaCIL), Department of Computer Science, Durham University, Durham, UK. [4]Computer Engineering Department, Middle East Technical University, Ankara, Türkiye. [5]Center for Robotics and Artificial Intelligence (ROMER), Middle East Technical University, Ankara, Türkiye. [6]Mechanical Engineering Department, Middle East Technical University, Ankara, Türkiye.
*Corresponding author. Email: thomas.schmickl@uni-graz.at
†These authors contributed equally to this work.
‡These authors contributed equally to this work.

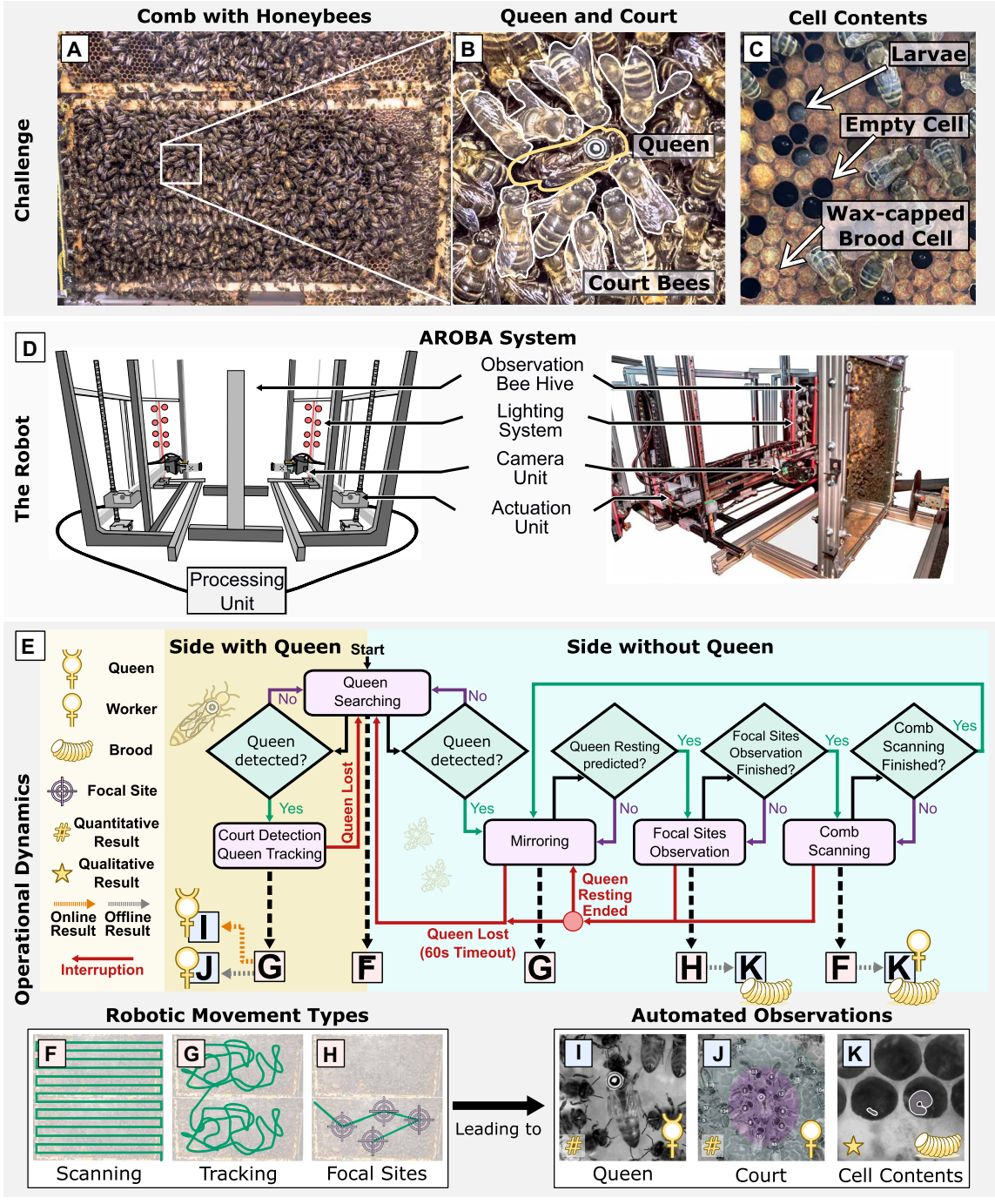

Fig. 1. The AROBA system is designed for autonomous focal observation and behavioral analysis in a honey bee colony. (**A**) Photograph of one side of a honey bee comb, with the queen and her court, surrounded by workers. (**B**) The queen (highlighted), marked with a fiducial marker, surrounded by her court (highlighted). (**C**) Photograph of a less crowded area of the comb showing different exemplary cell contents. (**D**) Schematic and photograph of the AROBA system, showing two modules placed on either side of the central observation hive. (**E**) Flowchart of the AROBA decision-making algorithm. (**F**) Generalization of movement trajectories of modules performing comb scanning operations for brood development monitoring and population level estimation. (**G**) Generalization movement trajectories of modules performing queen tracking and court detection. (**H**) Generalization of movement trajectories of modules performing focal site observation for brood development monitoring at target sites. (**I**) Exemplary image frame during queen tracking. (**J**) Visually highlighted court configuration with detected court bees. (**K**) Detail of comb cells with egg and larva highlighted.

From the late 18th century on, human observation has been the state of the art in ethology. For honey bees, this principle was pioneered by François Huber, who used specially designed observation hives in his work on honey bee behavior (*20*). Most prominently, the Nobel laureate Karl von Frisch (*21*) studied honey bees ethologically and, together with Nikolaas Tinbergen (*22*) and Konrad Lorenz (*23*), established ethology as a formal scientific discipline (*24*). Throughout the 20th century, ethological research relied on human observation and often qualitative behavioral analysis in laboratory settings (*25*, *26*).

For systematically observing animals in general and specifically honey bee colonies, robotics can be an important enabling technology allowing studies to go far beyond the possibilities of human observers in classical ethology. However, it is crucial that such robotic systems observe natural behaviors without producing behavioral artifacts. Table 1 provides a set of constraints and design directives that must be taken into consideration to perform technology-driven ethology. These guidelines have informed and guided our robot design to create an autonomous machine for ethological honey bee research by continuously collecting data for key behavioral metrics (KBM).

Recently, the deployment of fixed-camera systems coupled with automated image analysis has expanded research capabilities, improving data quality and objectivity and allowing for longer observation times (*27*–*30*). Advancements in automated honey bee tracking methodologies, pioneered by Feldman and Balch (*31*), have more recently been improved through convolutional neural networks (CNNs), thus enhancing automated (observer-independent) data collection and behavioral classification (*32*, *33*). However, such fixed-camera systems face a critical trade-off when capturing entire honey bee colonies between generating unmanageable amounts of data and missing important detailed interactions because of limited resolution. A dedicated subsection in the Discussion compares our Autonomous Robotic Observation and Behavioral Analysis (AROBA) system to other honey bee observation methods and technologies in the field, including "manual" observation methods that are common in bee ethology.

The key advantage of using a robotic system over a fixed-camera system is the presence of moving cameras on both sides of the hive in closer proximity to the comb. This offers multiple benefits: Mobile cameras can focus on what is currently important for the research, for example, continually creating close-up video recordings of the queen, of dancing bees, or of specific comb sections. This allows a higher image quality than fixed cameras, with more pixels capturing the specific area of interest. In addition, an AROBA system is slimmer than fixed-camera systems; thus, more hives can fit into the same laboratory space. This allows more repetitions of experiments and more control setups. Furthermore, the AROBA system actively exploits the fact that we observe processes that operate on different time and size scales in honey bee colonies: Fast-paced behaviors can be observed by continuous focus observations based on tracking individuals or groups, whereas interval-based sampling or scanning of the habitat for slow-acting processes is also possible. However, intermediate or mixed strategies can also be implemented, especially when multiple interacting robotic nodes are used. In addition, the AROBA system has autonomous zoom and focus functionalities, thus allowing detailed processes to be recorded at higher spatial resolution. Conversely, less zoomed-in images could be used for broader spatial observations. In conclusion, the AROBA system can precisely align with regions of interest in honey bee observations, eliminating the parallax problem, which often occludes the line of sight to each comb cell's content.

Table 1. Requirements and constraints in observing and systematically analyzing eusocial animal colonies. From these requirements and constraints, we deduced specific challenges in our robot design.

Design principles	General design imperatives (all animals)	Specific requirements for honey bee research	Challenges for robot design
Natural habitat	The animals should reside in an as-natural-as-possible environment to exhibit natural behaviors	A queenright colony with 1000+ worker bees, combs, and brood housed in an observation hive; ability to freely forage for food	Considering sufficient space for the observation hive, controllable entrance and exit access, and biocompatibility
Minimum disturbances	The stimuli produced by the observation system should not alter the natural behaviors of the animals	Honey bees are sensitive to visible light and environmental vibrations inside their hive	Using nonvisible light and minimizing the vibrations on the observation hive
Exhaustive coverage	The observational system should be able to cover the relevant habitat to prevent missing important behavioral aspects	The apparatus should cover the whole observation hive with honey bees and minimize the areas of occlusions	Maximizing the coverage area and fitting the robot dimension to the workspace limits
Long-term operation	The observational system should cover the habitat for periods long enough to allow interesting ethological or ecological observations	The apparatus should be sufficiently robust to observe the queen at least over a full brood cycle (21 days)	Ensuring the mechanism's lifetime, preventing unexpected failures and structural fatigue
Flexibility and versatility	The system should be able to observe, detect, and analyze many relevant specialized individual behaviors and general collective behaviors	The extracted qualitative and quantitative data should be derived from the queen, from workers, and from the comb-filling dynamics	Automatically recognizing and analyzing the observation objectives with sub-millimeter localization accuracy
Scalability	The system should be able to observe and quantify KBMs (see Table 2) on many different levels: population/colony level, group/cohort level, and individual level	The system should measure KBMs on the macroscopic level (colony-wide), mesoscopic level (groups), and individual microscopic level. Also, social interactions should be measured	Providing standard and efficient ways of data collection and retrieval with on-demand adjustable level of detail

Our specific honey bee–observing AROBA system can choose where, when, and at which resolution to perform the measurements to efficiently refine and complete the colony models. A plethora of methods for building maps that capture environment changes by autonomous robots have been successfully tested in human-populated environments (*34*). Such methods typically forecast the uncertainty of states and schedule the observations toward the most uncertain locations and times (*35*, *36*). Similarly, our AROBA system forecasts the changes in the queen's behavioral states and takes into account the combs' dynamics, choosing between scanning the colony contents or focusing on the queen. The priorities of our AROBA system to focus on either the queen or on the combs can be altered during the system's operation. In extreme cases, the focus can be on only tracking the queen, on comb scanning, or on continuous observation of specific focal comb areas (Fig. 1, D to K). Such modes of operation will likely improve the quality of these focal observations, but this will come at the expense of not sampling other relevant data in the hive context. In the study presented here, the system was set to provide at least five comb scans per day. If the queen was observed to be resting and we forecasted that she would likely rest for the next 10 min, then the robot on the other side of the hive would start to scan the comb. Whenever the queen started to move and the last scan occurred less than 8 hours ago, the scan was interrupted, and the actuator started to "mirror" the positions of the actuator on the queen's comb side. This is essential to more easily "catch" the queen in case she switches to the other side of the hive.

The main structure of our AROBA system is a gantry mechanism. Designing a gantry mechanism for observing honey bee behavior demands resolving several technical challenges. One of the primary challenges is ensuring a precise movement in a vertical plane parallel to the queen's movement plane. Additionally, the gantry mechanism must reliably and robustly carry the camera for continuous queen tracking. The design of high-precision linear actuators, including ball screws, supported by linear guides and driven by stepper servo motors is necessary to achieve the required precision and responsiveness. Our system's design addresses factors like stability and vibration control to prevent disturbances affecting the observation process. Furthermore, considerations for the hive environment and the behavioral characteristics of honey bees add layers of complexity to the technical challenges. Balancing these elements in the design process is essential to creating an effective and efficient gantry mechanism for studying queen honey bee behavior.

Here, we present an application of our AROBA system for continuous 24-hour-per-day observation of three main components of a honey bee colony (queen, workers, and the content of comb cells) and their interactions (Movie 1). The system can observe each of the three components at different spatiotemporal resolutions using infrared (IR) cameras with controllable focus and focal length attached to robotic actuators. Our AROBA system cannot observe the entire honey bee colony all at once with maximum resolution. Rather, observations of different colony elements are performed according to the priorities of the conducted study, for example, focusing on the queen's movement rather than the comb dynamics. This enables the generation of high-quality datasets that exceed the existing amount of consistently recorded observations of tracked and classified queen behaviors currently reported in published systems (*27*). Our system tracks not only the queen and the workers but also the development of the eggs that the queen lays, as well as other elements, such as nutrients deposited in the comb cells. These data also provide essential indicators of colony health and predictors of future colony growth.

The well-being of a honey bee colony is highly dependent on its queen and on her interactions with workers and combs. Therefore, we have designed our AROBA system to collect data at multiple system levels to quantify important colony KBMs. We distinguish whether the KBMs provide information about the queen, her court of adult workers, or the wax combs and the brood in their cells. We further distinguish between processes operating at the microscopic (individual, short-term, local proximate), at the intermediate mesoscopic (group-level, medium-term, semi-local, social), or at the macroscopic (aggregated, long-term, global, ultimate) system layer. Furthermore, KBMs related to interactions between different types of agents are

Movie 1. Video overview of the developed methodology (robots and algorithms) and housing of the bees. The video briefly shows the key results of our system, as well as exemplary image streams produced by our system.

addressed, for example, social interactions between the queen and worker bees or between the bees and brood. A nonexhaustive list of KBMs derived from data collected by our AROBA system is shown in Table 2.

RESULTS

To demonstrate the capabilities of our AROBA system, we present information on the data obtained during 1 month of system operation. The results are organized according to the structure shown in Table 2. Figures 2 to 4 show automatically derived quantitative KBMs and qualitative data, which still require human postprocessing for quantification, on all four system levels, as they are listed in Table 2. Statistical hypotheses are described in table S5.

Data obtained

The AROBA system was set up in July 2023, and data were collected 3 months later in September 2023. The AROBA system operated autonomously, tracking the honey bee queen and scanning the contents of the combs. From 20 September 2023 to 19 October 2023, the AROBA system collected 27.4 million images of the queen and her surroundings, including 9789 egg-laying candidate locations. The system produced 657 continuous queen tracks, with the longest track lasting for 6 hours and 56 min, capturing 25.6 m of queen movement. There were 161 tracks that took longer than 1 hour and contained 74.3% of the detections of the queen and 161 tracks shorter than 5 min, which contained only 1% of the detections. The system captured 201,173 snapshots of the combs at 67-μm/pixel resolution, 96,169 images of the combs at 34-μm/pixel resolution, and 101,831 images at 25-μm/pixel resolution.

The recorded data were used to create two datasets. The first dataset consisted of a 24-hour recording performed on 10 October 2023 (the day with the most queen detections), containing 4.9 million images with 1.2 million queen detections and 196 million worker bee detections. The second dataset consisted of data recorded over 1 month from 20 September 2023 to 19 October 2023, containing the data presented in the previous paragraph.

Monitoring the honey bee queen

To enable additional insights into the system's capability to collect data on the honey bee queen, we provided data gathered over a 24-hour period. During this time, the system operated completely autonomously without any human intervention. The queen was tracked by our AROBA system for 19 hours and 32 min, corresponding to 81.4% of the observed time, producing 1.2 million queen detections. Interruptions in tracking were caused by the queen moving behind obstructive elements. Our system observed, detected, classified, and quantified a substantial set of KBMs of the queen.

As a macroscopic KBM, our system observed the queen's spatial coverage of the hive over time. The queen was found to spend 75% (left comb side) and 90% (right comb side) of her time in 15% and 36% of the total hive space, respectively (Fig. 2B). The queen exhibited a strong preference for specific resting sites, spending disproportionately more time at these preferred sites during resting periods than at the rather dispersed sites traversed during her active walking phases (Fig. 2B). The queen also showed a strong preference for resting on the left side of the comb, where she spent 11 hours and 38 min, compared with the right side, where she rested for 3 hours and 14 min. The preferred resting area (orange rectangle in Fig. 2A) was chosen 657 times out of 1793 resting events on the upper comb, thus in 37% of resting cases in an area that accounted for only 16.67% of the total upper comb area. A more detailed analysis of this spatial preference for the queen's resting periods is given in Fig. 5.

As a mesoscopic KBM, the first passage time was analyzed by our system (Fig. 2C). When looking at the differences between the right and left sides of the hive, we could see a slight difference in the means (on average 20 s), which we assumed does not have much biological relevance given the spread of the first passage values. The upper bounds of the time ranges grew faster than the observed mean or the minimum values as the displacement threshold reached the physical size limits of the comb space (Fig. 2D).

At the microscopic level, our system extracted the queen's position, orientation, and speed over time (Fig. 2, E to G) and aggregated these data into continuous tracks. The reconstructed single-day trajectory of the queen consisted of 14 tracks ranging in length from

Table 2. KBMs autonomously measured by our AROBA system. The system observes, detects, classifies, and quantifies 23 event types across macroscopic, mesoscopic, microscopic, and social interaction layers. KBMs that are automatically quantitatively measured by our system are indicated with an asterisk (*); those that are collected as qualitative-only data (so far) and those that require manual quantification are marked with a dagger symbol (†). More details on the KBMs, their evaluation, and their significance are given in the Supplementary Materials ("KBMs - Definitions and Significance" and table S4).

Type of KBM	Queen	Workers	Brood and comb
Macroscopic	A1*: Areal coverage of comb space over time	B1*: Density and numbers of bees detected	C1a*: Global egg position map
			C1b*: Overall egg-laying rate
Mesoscopic	A2*: First transit time of the queen	B2*: Worker densities near and far from the queen	C2*: Compactness of the queen's egg-laying pattern
Microscopic	A3*: Queen positions, locomotion, and orientations	B3*: Worker positions, locomotion, and orientations	C3a†: Successful brood development
			C3b†: Failed brood development
Social	A4a†: Feeding the queen	B4a†: Cleaning the queen	C4a†: Nursing
			C4b†: Hatching
	A4b†: Cleaning the queen	B4b†: Worker trophallaxis	C4c†: Capping
			C4d†: Worker inspection
	A4c*: Court dynamics	B4c*: Time spent in court	C4e†: Queen inspection
			C4f†: Egg-laying events

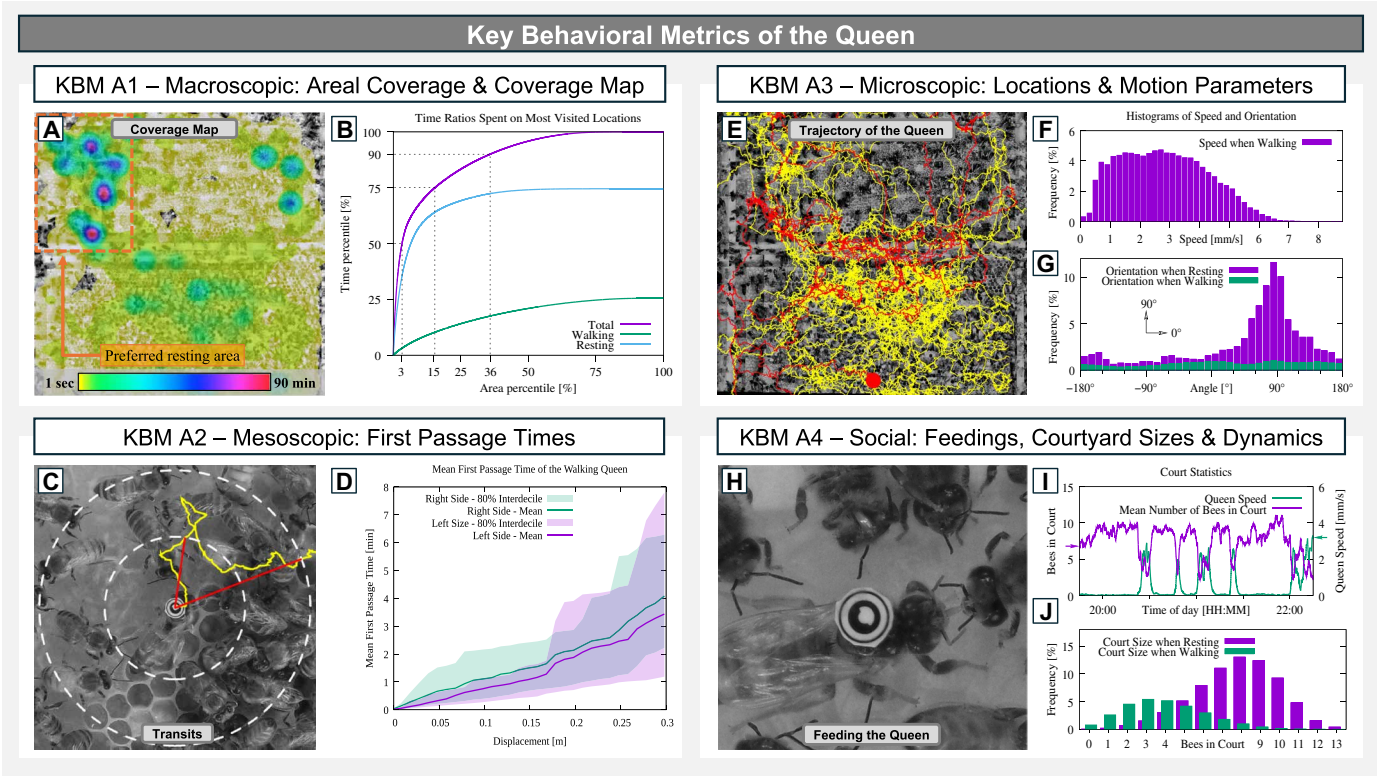

Fig. 2. Representative queen-related KBMs autonomously observed by our AROBA system. (**A**) Map of the area covered by the queen on one side of the hive. A vicinity of 20 mm around the queen is considered to be visited, thus potentially affected by the queen via pheromones and vibrations. The left third of the upper comb on this side of the hive (see orange rectangle) is considered to be a preferred resting area. (**B**) Proportion of the queen's total time spent on the covered area of each side of the comb, together with the percentage of time she spent on a given area during resting and walking. (**C**) Example sketch of first passage time estimation with the queen's trajectory in yellow and example displacement thresholds in red. (**D**) Observed first passage times of increasing displacement thresholds for both hive sides, showing mean and 10th/90th percentile range. (**E**) Stitched still image overview of one side of the observation hive with the observed queen's trajectories. The image was composed using odometry-based stitching. The last continuous track of the dataset is shown in red; all others are in yellow (movie S1). (**F**) Distribution of the queen's walking speed with a histogram bin size of 0.2 mm/s. (**G**) Distributions of observed queen resting and walking orientations with a 10-degree histogram bin size. (**H**) Representative frame of recorded queen feeding events (movie S2), captured at our highest possible image resolution. (**I**) Two-hour court data sample analysis, correlating the queen's speed with her court size. (**J**) Distribution of court sizes. The tracking performance was evaluated on 16,230 manually annotated images, 6414 of which contained the queen. The average error is 0.847 pixels (56.7 μm) with a maximum value of 2.23 pixels (149 μm). The precision is 1.0, the recall is 0.952, and the F1 score is 0.975. In the analyses for (B), (F), and (G), the queen's state changes from resting to walking at 1 mm/s and reverts to resting when the queen fully stops.

0.01 to 12.1 m and lasting from 8 min to 4 hours. More than 80% of detections were contained in four tracks with lengths exceeding 100 min each. The total observed distance of the queen's movements was 67.12 m, with 34.95 m traversed on the left side and 32.17 m on the right. The 1.2 million queen orientations extracted indicated that the queen spent more than 50% of her resting time in an upward ±25° orientation (Fig. 2G). We compared the empirical distributions of queen orientation when resting and walking in Fig. 2G to the uniform distribution. A Kolmogorov-Smirnov (KS) distance of 0.11 for walking and 0.40 for resting shows that queen orientations were less uniform when resting. The 10th percentile of queen speed was 0.9 mm/s, and the 90th percentile was 4.8 mm/s. The median speed was 2.7 mm/s, and the mean speed was 2.8 mm/s (Fig. 2F).

Regarding the queen's social interaction metrics, the system could detect, count, and track the court bees within a certain distance from the queen. See Fig. 3 for more details regarding those measurements. Our 1-day dataset provided us with 717,223 court bee counts. The number of bees directly interacting with the walking and resting queen is shown in Fig. 2 (I and J). While resting, the number of court bees was between 5 (10th percentile) and 10 (90th percentile) with a median of 8 bees and an average court size of 7.8 bees. The number of court bees at any given time of queen movement was between 1 (10th percentile) and 7 (90th percentile) with a median of 4 bees and an average of 3.9 bees.

Monitoring adult worker bees

In addition to tracking the queen, our AROBA system could detect individual adult worker bees on and in the comb cells. When the queen was resting, the system could stop tracking her and start to systematically scan the comb while detecting and localizing the other bees in the colony.

As a macroscopic metric of the worker population, we estimated the worker bee density over the entire comb area (Fig. 3A). Moreover, the number of bees detected on each side of the hive during a day allows us to estimate the overall population of the hive (Fig. 3B). During the 1-month period of operation, the system performed 1811 scans, providing 151,996 images with more than 4.8 million worker bee detections. These detections allowed us to estimate the

colony population growth from 2350 adult bees on the 20th of September to 3350 adult bees on the 19th of October. We found a statistically significant difference between the number of bees on the left and on the right side of the hive, yet the average difference between the daily population sizes of the month-long dataset (Fig. 3B) on each side amounted to only 5.2%.

As a mesoscopic KBM, a worker bee detection algorithm was performed in parallel with the queen tracking algorithm to measure the density of bees around the queen. The data gathered over 1 day (5.1 million detections) indicated that when the queen did not move, the density of bees in her immediate vicinity—we call this area the "court interaction area" (Fig. 3C and movie S3)—was between 0.5 and 1.0 bees/cm^2 (10th/90th percentile) with an average of 0.78 bees/cm^2. A wider area around the queen, called the "outer court area" (Fig. 3C), was less densely populated: 0.62 bees/cm^2 compared with the rest of the comb with 0.37 bees/cm^2. The 10th/90th percentiles were 0.38/0.90 bees/cm^2 and 0.21/0.55 bees/cm^2, respectively (Fig. 3D); this difference in densities is shown in detail in the Supplementary Materials (table S5).

To measure the effect of the queen's presence on bee density, we also looked at how many bees were around the queen compared with the other (queen-less) side of the hive. On average, there were 5.1 more bees on the queen's side in a 130 cm–by–72 cm area centered around her than on the other side. As a microscopic KBM, we processed 97 million bee detections gathered over 1 day to obtain the bee speed distribution. Worker bee walking speed and resting orientation differed more from the queen than the orientation while walking. This is shown in distribution distances of KS = 0.29, 0.25, and 0.09, respectively (Fig. 3G).

To measure the queen's social connection with worker bees, we determined the typical duration of worker-queen interactions by extending the worker bee detection with an algorithm that allows further tracking of the unmarked workers. Our analysis of the 26,082 tracks collected over 1 day revealed that about 97.1% of direct worker-queen interactions were shorter than 1 s. However, of the 2.9% of events where interactions were longer than 1 s, 8.5% of workers resided close to the queen for more than 30 s (Fig. 3J).

Monitoring the brood status and the egg-laying patterns on the combs

A key feature of our AROBA system is its capability to monitor the brood status by analyzing the development of the comb structure through the queen's oviposition behavior. This analysis was facilitated by a CNN that classified the queen's oviposition behavior [more

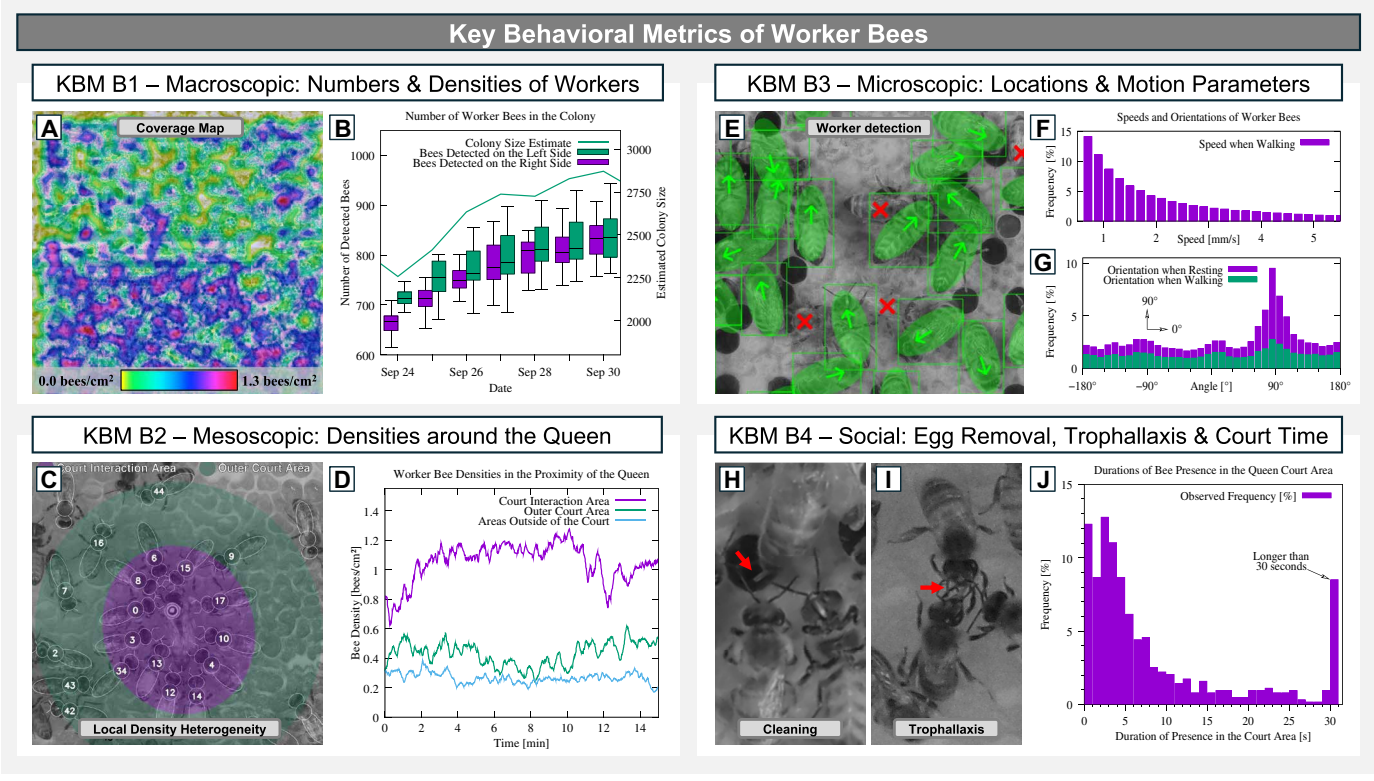

Fig. 3. Representative worker-related KBMs autonomously observed with our AROBA system. (**A**) Worker population density across the left comb. (**B**) Number of detected bees on both sides of the hive during a day along with an estimate of the total number of bees in the colony. The total number of bees was estimated from the sum of both sides, as well as the precision and recall of the detector. The precision was 0.89 (n = 6994 detections), the recall was 0.47 (n = 13,189 annotations), and the F1 score was 0.62. (**C**) Court bee detection and tracking in the queen's vicinity (movie S3). (**D**) Worker bee density near the queen. Detection of crawling, unobstructed bees in central regions of the hive, which correspond to Fig. 2 (D and I), has a precision of 0.82 (n = 3886 detections), a recall of 0.84 (n = 3804 annotations), and an F1 score of 0.83. (**E**) Representative image for worker bee detection. Green ovals, true positives; red crosses, false negatives; arrows, worker bee orientations. (**F** and **G**) Distributions of worker bee speeds and orientations. (**H**) Worker bees removing an unwanted egg that got stuck on the queen's abdomen, thus cleaning her (movie S4). (**I**) Worker bees sharing food trophallactically (movie S5). (**J**) Distribution of the duration of worker bee presence in the queen's court.

details are given in the Supplementary Materials section "Measuring the Oviposition Rate (Egg-Laying Rate) of the Queen"].

As a macroscopic KBM, we systematically recorded the spatial distribution of oviposition events over the entire comb area (Fig. 4, A and B) from the 30-day dataset, beginning 20 September 2023, with a maximum of 350 eggs and a minimum of 46 eggs laid per day (considering the universal time zone for daily intervals). The 10th percentile and 90th percentile of the number of eggs laid were 96 and 296, respectively. The mean number of eggs laid per day was 187, with no apparent preference for either side of the hive (Fig. 4A). When applied to a dataset of 9789 candidate oviposition events, the CNN-based method identified 5961 oviposition events (Fig. 4B). For details on the training and testing of the CNN, see the description in Fig. 4 or the Supplementary Materials ["Measuring the Oviposition Rate (Egg-Laying Rate) of the Queen"].

As a mesoscopic KBM, the oviposition compactness was analyzed by our system (Fig. 4C). This was achieved by assessing the brood occupancy status of neighborhood "ring" sizes of $r = 1$ containing 6 cells, $r = 2$ containing 12 cells, and $r = 3$ containing 18 cells, corresponding to blue, green, and violet zones, respectively, in Fig. 4C. Our system systematically observed that more than 50% of the oviposition acts happened in regions where one or more eggs were recently laid in one of the six neighboring cells. More than 50% of these egg-laying acts also occurred in regions with two or more recently laid eggs within a radius of three cells (Fig. 4D).

As a microscopic KBM of brood development, we observed larval growth within brood comb cells. Successful brood growth began with the queen laying a single egg into a cell. A larva then emerged after 3 days (Fig. 4E, i to iii). This larva was then fed, and it grew to fill the entire cell at an age of approximately 3.5 to 4.0 days (Fig. 4E, iv and v). Typically, successful larval development was marked by the capping of the cell about 5 days after hatching from the egg (Fig. 4E, vi). Conversely, cases of unsuccessful brood development ("brood cannibalism") occurred when an egg or the subsequent larva was eventually removed. This removal resulted in an empty cell, and the predicted cell capping did not occur (Fig. 4F, i to vi, and movie S8).

For observing social interactions, our system captured a plethora of key behaviors regarding interactions between the queen, workers, and brood. Currently, our system does not extract quantitative data autonomously from those qualitative video recordings. However, because we know the egg-laying positions and time, we can forecast such events and set locations of interest that the robot monitors frequently. We captured interesting events and qualitative data from the video stream. Figure 4G shows a representative set of interactions between different types of agents: brood nursing by workers (Fig. 4G, i), workers capping fully grown larvae with a wax cover (Fig. 4G, ii), workers helping fully grown adults hatch from underneath their wax-capped cells (Fig. 4G, iii), general brood inspection acts of workers (Fig. 4G, iv), oviposition acts by the queen (Fig. 4G, v), and

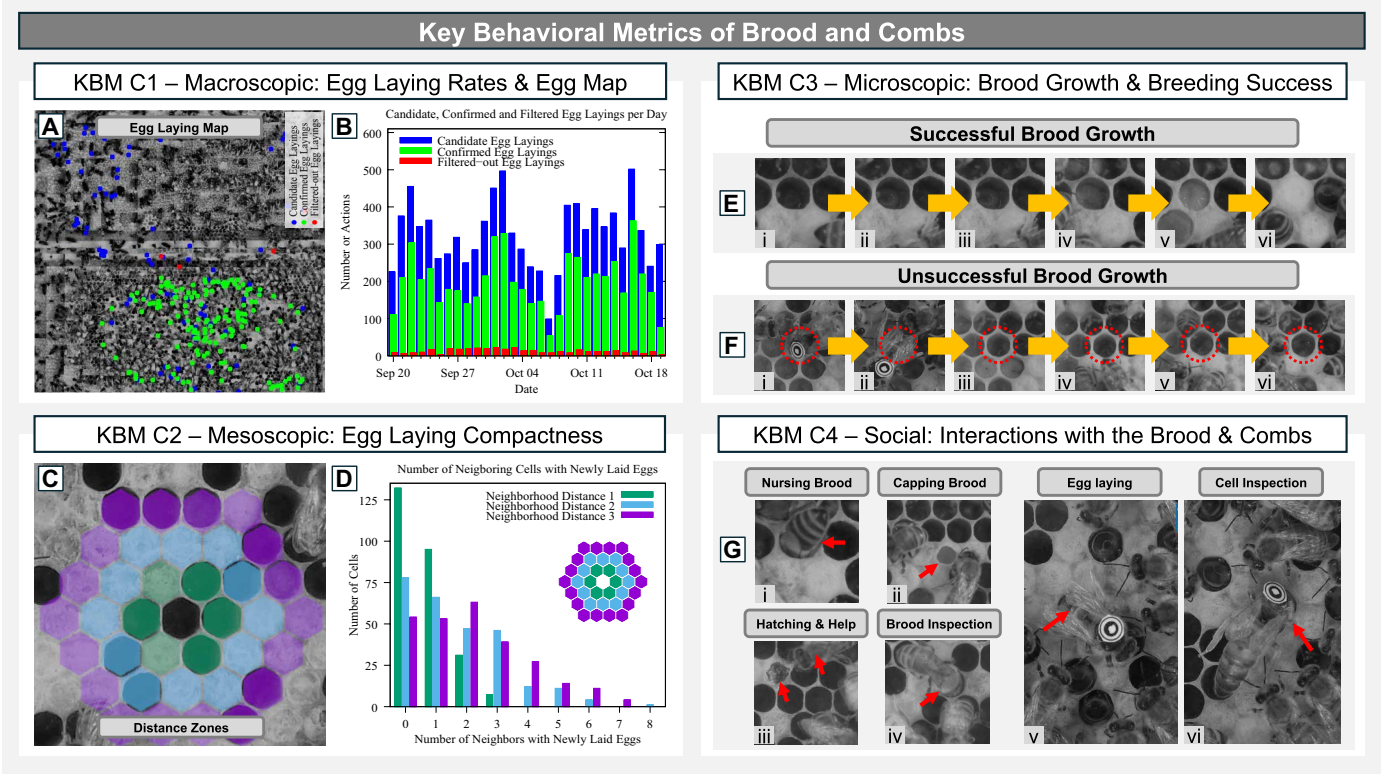

Fig. 4. Representative comb-related KBMs autonomously observed with our AROBA system. (**A**) Positions of the candidate, the confirmed, and the filtered egg-laying acts over 1 day (movie S6). (**B**) Candidate and confirmed egg-laying acts over 1 month. (**C** and **D**) Metric indicating the spatial compactness of the egg-laying acts over 1 day. (**E** and **F**) Successful and unsuccessful brood growth examples (movie S8). (**G**) Worker bees interacting with the brood cells (movies S9 and S10) and details of the honey bee queen inspecting comb cells and laying eggs into them (movie S7). A CNN for oviposition detection was trained on data obtained from queen tracking ($n = 22{,}715$ images) and tested on independent data from queen tracking ($n = 408$ image stacks), resulting in a precision of 0.9338, a recall of 0.9513, and an F1 score of 0.9425.

cell inspections by the queen to find suitable cells for egg laying (Fig. 4G, vi).

We further analyzed our data to characterize the queen's resting behavior. As indicated in Fig. 2A, our data suggested a "preferred resting zone" on the upper comb. Figure 5A shows that our observation strongly differed from the resting time distribution found in another model insect species [*Drosophila melanogaster*; reference data from (*37*)]. The gray area indicates the whole envelope of observations in *Drosophila* (male and female, in light and in darkness) between the lowest and the highest observed resting time probabilities. Although in the brood nest area (magenta line) the resting time of the queen fell within the "envelope" of reported *Drosophila* observations at short resting events ($d \geq 30$ s), this only happened for very long resting times ($d \geq 3000$ s) in the other hive areas (orange, cyan, and blue lines). The observed behavior in the presumed preferred resting zone differed also from the resting behavior (orange line) in the lower comb's periphery region (blue line) and in the other regions of the upper comb, which were also used for honey storage (cyan line). In the preferred resting zone (Fig. 5B, orange), which is the upper comb area, we found that the queen rested longer and more often, following the same general distribution pattern as her resting that occurred in the other honey storage areas but strongly deviating from her resting behavior in the brood nest area (Fig. 5A). Very short resting events ($d < 12$ s) were similarly frequent in all regions of the hive (Fig. 5A). There was generally a preference for peripheral areas of combs for the queen to rest; however, this phenomenon was the strongest in the presumed preferred resting zone indicated by the orange area in Fig. 5B. This localized preferential resting was not a short-term phenomenon (Fig. 5C). We normalized the daily sum of all resting periods on the upper comb to compensate for the size differences of the investigated areas. We found that for 24 of 30 days this resting zone was spatially preferred, in most cases to a high extent. For the remaining days, when such a prominent preference was not found, the overall resting of the queen was comparably short. It is also noteworthy that we observed resting rates per day that varied almost one order of magnitude among these days, from a minimum resting of 1.47 hours per day to a maximum resting of 11.76 hours per day. Specific details on the data processing for producing Fig. 5 are given in the Supplementary Materials ("Data Processing and Statistical Methods").

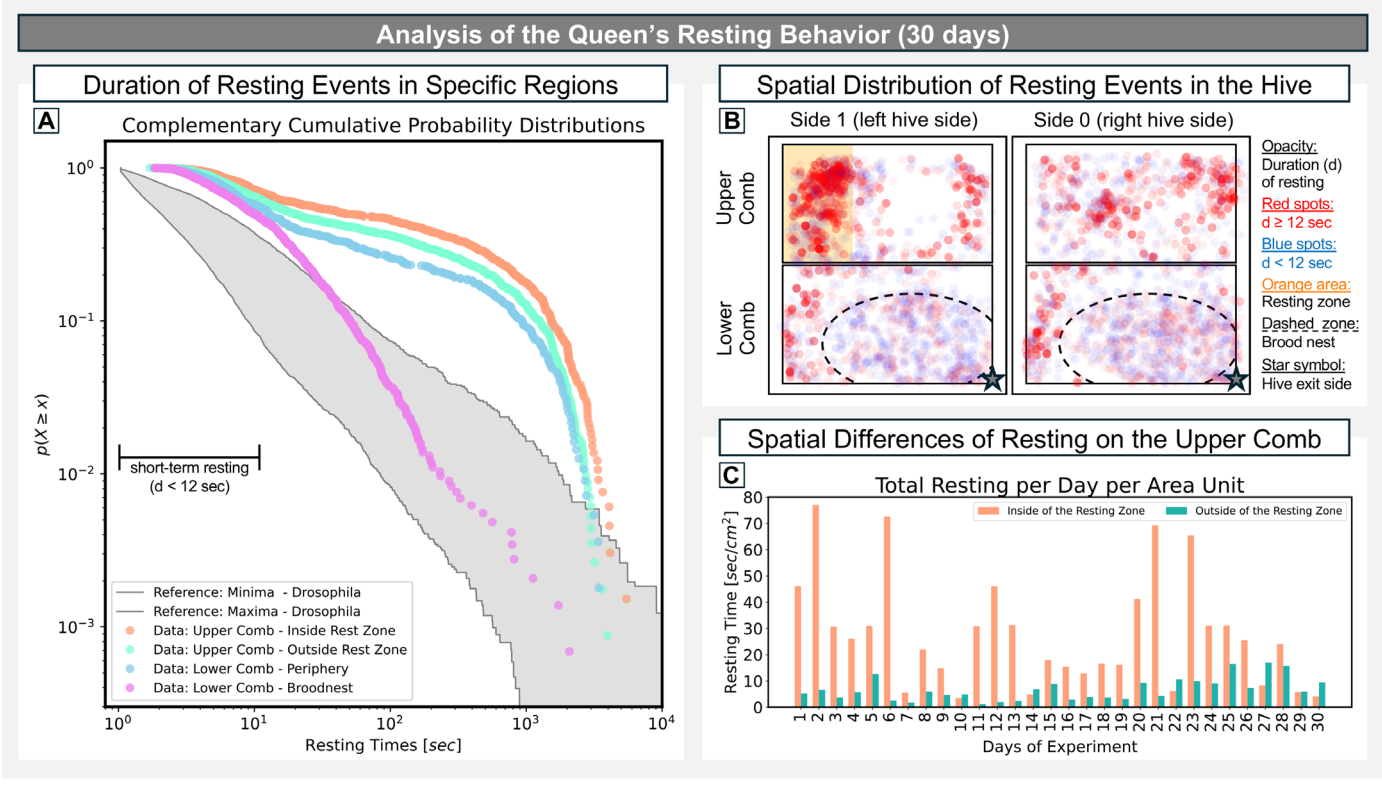

Fig. 5. Analysis of spatiotemporal aspects of the queen's resting behavior. (**A**) Complementary (inverse) cumulative probability distribution of the queen's resting behavior over 30 days of observation. Locomotion pauses of the queen shorter than 1 s or that fall within a time window of 10 s before an egg-laying event (most likely cell inspections, see also movie S7) are excluded from this dataset to focus on the queen's resting behavior. The orange area shows the presumed preferential resting zone. The cyan area shows the other areas of the upper comb. The magenta area shows the area that we identified as the brood nest region on the lower comb in Fig. 2A. The blue area shows the remaining (periphery) region of the lower comb. The gray area shows the envelope between the reported minimum and maximum in reference data from literature (*37*), indicating resting data of *Drosophila* fruit flies. (**B**) Spatial map of the queen's resting locations in the hive. Red circles represent resting events longer or equal to 12 s. The blue area shows the resting phases below 12 s of duration. The shades of color indicate the duration of resting phases: 10% base opacity + 80% opacity linearly stretched between the minimum (1.7 s) and the maximum (1.52 hours) observed resting phase. The orange area indicates the resting area, as also shown in Fig. 2A. The clipped elliptic dashed line indicates the outer rim of the brood nest region in our colony. The star indicates the hive's entrance/exit location. (**C**) Comparison of total resting periods per day in and outside the presumed preferred resting zone on the upper comb split into two datasets: inside versus outside of the orange-indicated preferred resting zone, normalized in s/cm^2.

DISCUSSION

We present here an AROBA system specifically tailored for autonomous long-term observation of honey bee colonies. We have demonstrated the versatility and utility of this system through automatically collected datasets and algorithms that are capable of directly extracting 23 KBMs of the honey bee colony (see Table 2 for a list) either directly from the motion trajectory of the robot (e.g., the queen's coverage of the hive or the queen's resting locations) or via the extraction of KBMs from the recorded video footage (e.g., egg-laying rate or the sizes of the court bee group). These KBMs measure the honey bee colony functionalities on four different levels: the macroscopic, the mesoscopic, and the microscopic system layers and on the social interaction layer. More details on these KBMs, their evaluation, and significance are given in the Supplementary Materials ("KBMs - Definitions and Significance" and table S4).

Although some data are shown here qualitatively, others were automatically extracted quantitatively. The system has demonstrated its ability to track long-term colony-wide trends, such as the colony size evolution, while also providing detailed long-term insights into spatial and temporal patterns within the colony, such as the queen's oviposition behavior and the spatial coverage of the hive during her patrolling activity. The latter is important for pheromone dispersal (*38*, *39*).

Health of the colony and avoiding behavioral artifacts

Our AROBA system was designed to minimize its influence on the honey bees' natural behaviors and well-being. This includes features such as adequate ventilation, provision for supplemental feeding and medication, and the use of illumination outside the bees' visual spectrum to maintain a dark environment similar to a natural beehive. Although the bees could freely fly out to perform their foraging activities, the hive and the robotic system were housed in a temperature-controlled laboratory to prevent the heat generated by its electrical components from influencing bee behavior. Substrate vibrations play a pivotal role in honey bee communication and colony organization. It was therefore of the highest importance to minimize the vibrations caused by the systems' motors, as well as the transmission of potential vibrations to the hive. Detailed information on the design choices made to avoid influencing the natural behaviors of the animals is provided in the Supplementary Materials ("Hardware of our AROBA System," "Design Decisions for Preventing Behavioral Artifacts," and "Detailed Specifics of the Mechatronics Design"). The prolonged observation did not adversely affect the health of the colony, as evidenced by the substantial increase in population size during the observation period (Fig. 3B). This growth indicated not only prolific egg laying by the queen (Fig. 4, A and B) but also successful development of the brood into workers and suggested a high survival rate of adult workers, contributing to the rapid expansion of the colony. Further information on the long-term health of the study colony is provided in the Supplementary Materials ("Long-term Effects on Colony Health and Behavior").

Unexpected observations and biological findings

Although our ethological experience suggested that a queen tends to rest in the upper areas of the observation hive, where the honey stores are usually located, we were surprised by the consistency with which our queen chose specific resting locations. The majority of resting events occurred in the left part of the upper comb on the left side of the hive (Fig. 2A, bright spot and rectangular area). This resting spot preference warrants further investigation into the local factors influencing the queen's decision-making. The entire upper comb was used by the colony as a honey storage area, and the indicated resting zone was the furthest distance away from the hive's exit/entrance and thus likely the safest and quietest place in terms of worker bee traffic in the hive. On the basis of the 30-day-long observation that we analyzed in Fig. 5, we found strong evidence that this hive area is, in fact, preferred by the queen. Across the whole spectrum of resting durations longer than 12 s, this area exhibited the highest frequency of resting events (Fig. 5A). Although other non–brood nest areas showed similar distribution patterns, longer resting events were less frequent in these areas. This behavior was observed on most days throughout the 30-day observation period.

Figure 5 reveals two additional key findings. First, the queen's resting behavior differed notably between the brood nest and non–brood nest areas, even excluding short resting events associated with egg laying (likely cell inspections, see also movie S7). This finding suggests that the queen exhibited distinct activity modes within and outside the brood nest area. Second, the resting time distributions for events lasting between 1 and 12 s were consistent across areas, suggesting that these were brief pauses due to hive traffic rather than recuperative rest. Our data indicate that the density of bees, and thus the difficulty of navigation, was relatively consistent across different regions of the hive. In our interpretation, we distinguish between short-term motion pauses ($d < 12$ s) and longer resting periods ($d \geq 12$ s), as shown in Fig. 5B. Future research is needed to further investigate the characteristics of resting and motion in the beehive. As we demonstrate here, our AROBA system can provide the relevant data in sufficient quantity and quality for such endeavors.

Furthermore, the queen preferentially orientated herself vertically upward (90° ± 25°, median ± interquartile range) during 50% of her resting time, whereas her orientation during walking periods was evenly distributed (Fig. 2E). During the 1-month-long period of monitoring, the queen walked almost the same distance on both hive sides (746.78 and 751.23 m), a result that supports our alternate tracking-and-scanning regime. However, she spent 59% of her time on the left side (side 1) of the hive.

The quantitative data presented in Fig. 2 (B and D) provide interesting insights into the queen's exploration versus exploitation trade-off: balancing the distribution of footprint pheromones throughout the hive with the need to lay eggs in a compact brood nest for efficient thermoregulation by worker bees. In parallel, our AROBA system provides detailed data on the microscopic properties of these locomotion behaviors (Fig. 2, F and G), the dynamics of the court bees (Figs. 2, H and I, and 3J), and the resulting patterns at various system levels (Fig. 4, B and D).

Limitations of our system

A principal limitation of our AROBA system is its inability to observe all colony states simultaneously. The system must prioritize observations on the basis of the likelihood of changes in specific states of the observed system, necessitating the use of temporal models to predict future events. However, there is no mechanism to verify whether the estimated rate of change is slower than the actual rate of change in the colony, because the scheduled observations might not capture all relevant events.

Additionally, the system relies on maintaining high visual transparency of the hive's glass cover. Fogging due to microclimate differences and wax deposition by bees can impair the performance of vision algorithms. However, our system's moving camera can proactively address

this issue by repositioning itself to view areas of interest through clearer sections of the glass. Although frequent cleaning can further mitigate this problem, it can also disturb the colony and potentially trigger unnatural behaviors. More information on glass treatment and a quantitative analysis of glass decay in our study is provided in the Supplementary Materials ("Glass Treatment"). Additional considerations regarding the potential limitations of our system are discussed in the Supplementary Materials ("Extended Discussion").

During the 30-day recording period, the AROBA system achieved 97.6% uptime but encountered some challenges that required maintenance intervention. On two separate occasions, bees escaped the hive and obscured a calibration pattern, necessitating their removal to resume system operation. In another instance, a small gap in the hive was discovered and sealed. Sensor drift in the actuator caused issues in calibration pattern detection on two occasions, which were resolved remotely through software updates. A thorough cleaning of the hive's glass cover became necessary at one point during the 30-day period of observation.

Technologies for monitoring, observing, and tracking animals

Our AROBA system was carefully designed to minimize its influence on the observed honey bees. This allows for the study of natural behaviors without introducing experimental artifacts. Although the literature on animal-observing robots is rather limited, there are examples that show that such systems typically need to be either well hidden (as is the case in our study) or biomimetic to avoid disturbing the animals.

Prominent examples of observation-only robots in wild habitats include the nonbiomimetic MesoBot, which tracks marine organisms in the deep sea (*40*), and various biomimetic robots designed to observe oceanic life (*41*, *42*). Aerial drones have also proven effective for wildlife monitoring, often outperforming human observers in localization and counting tasks (*43*). Thermal sensing from drones has further enhanced wildlife observation capabilities (*44*).

Although our AROBA system was deployed indoors, it observed a complete honey bee colony that successfully overwintered and foraged freely in the outdoor environment. Thus, we consider our AROBA system to be operating in at least a "semi-wild" setting. Compared with the aforementioned systems (*40*–*44*), our AROBA system demonstrates high flexibility, versatility, autonomy, and long-term operation capabilities.

Smart beehives represent a different technological approach for monitoring honey bees in the wild, sensing mostly on the macroscopic (colony) level. These systems are either specifically designed hives with technological augmentations (*45*) or modules added to existing standard hives (*46*). They typically use sensors to measure in-hive climate parameters like temperature, humidity, and CO_2 and O_2 levels (*46*, *47*). Other approaches use acoustic monitoring to assess bee activity and potential swarming behavior (*46*, *47*). Additionally, weight dynamics of the hive can be tracked to estimate honey yield (*47*, *48*). Our AROBA system differs strongly from these technologies, because it is designed for fundamental research in behavioral biology and therefore collects data also on the mesoscopic and microscopic system levels. It also incorporates autonomous mobile robotic components, which are not typically found in "smart beehives" that are currently on the market.

Comparison with other technologies and methodologies

The classical methodology for observing honey bees relies on visual observation by human researchers. Most studies have focused on worker bees, with systematic visual observations of the queen being rare. One example study was based on a single 5-hour continuous observation of the queen and a few continuous observations of court bees (*49*). Another study reported 14 queen-focused observations, the longest lasting more than 115 hours (*50*). However, the latter primarily used interval-based sampling in 3- to 8-hour intervals. These long-term observations were made with 100 to 700 bees—a colony size that would not survive winter. Two seminal studies observed queens and their court bees in mid-sized colonies (2500 to 10,000 bees) for 1 hour per day (*19*, *51*). Another study observed the queen over 33 days, with two daily 2-hour continuous observations in a colony of approximately 13,000 bees (*52*).

Generally, the human factor is a limiting factor in ethology. Long observations are tiring, ultimately resulting in poorer data quality. Although increasing the number of observers may compensate for fatigue, the added heterogeneous subjectivity within the observer pool may decrease data quality again. In contrast, our AROBA system enables autonomous and continuous queen observation 24 hours per day, with the potential for unlimited duration given sufficient maintenance and data storage. Herein, we report robotic observations in a full-sized, healthy colony that successfully overwintered. More details are given in the Supplementary Materials ("Long-term Effects on Colony Health and Behavior"). Additionally, our system autonomously observed comb states, worker states, and worker densities.

Our AROBA system presented here was specifically tailored to focus on honey bee queen behavior. The literature reports several technologies focusing on other aspects of honey bees. Visual observation with fixed-mounted cameras was used to track worker bees with "barcodes" mounted on them (*32*, *53*), sometimes to extract social networks of interactions between worker bees (*54*–*56*). Markerless tracking of worker bees across the colony using fixed cameras has also been reported (*29*, *57*–*59*).

The downside of fixed-camera systems that capture the whole hive side is that either they reduce the number of pixels that represent one bee or they require expensive high-resolution cameras, which also dramatically increase the data load. Additional problems are often caused by the decay of glass transparency and potential reflections from lamps. When looking into the comb cells becomes important, the "parallax problem" (most cells are seen from the side and the cell floor is not visible) occurs strongly with fixed cameras. Moving the camera further away from the hive can alleviate the parallax problem, but it increases the space requirements of such systems. Wide-angle lenses may allow the camera to be closer, but the parallax problem and distortions will increase. A potential compromise is using multiple cameras focused on specific regions, as demonstrated in a study with a three-camera array (*60*). However, such solutions pose challenges like increased power consumption, heat dissipation, space requirements, and algorithmic complexity, particularly in handling object transitions between different camera views.

In the literature, video recordings with fixed cameras have also been reported for observations of a small subset of a brood (*61*), for waggle dancing bees (*28*, *62*, *63*), and for forager bees in their homing flights (*64*–*66*). Besides visually tracking bees in hives, methods based on radio frequency identification have also been used (*67*), mainly at the hive's entrance/exit (*68*, *69*). Although using such transponders inside the hive may reduce problems associated with the glass of an observation hive, they will have very limited use in observing and discriminating behaviors and brood states.

There is no clear, easy solution when designing an observation system with fixed cameras because the more they are tailored for one aspect, the less they seem suitable for others. We believe that our

AROBA system comes closer to an effective solution because it can operate with a modest camera, requires only one camera per hive side, and can focus on specific animals while surveying the whole colony on the other side of the hive. It minimizes the parallax problem and avoids problems with reflections by positioning the camera close to the glass. Additional considerations about similar technologies are provided in the Supplementary Materials ("Further Comparison to the State of the Art").

Conclusion and future potential

We envision further developments of our AROBA system that will allow us to deepen our understanding of the self-organization processes governing honey bee colonies. Aggregated and complex KBMs, combining multiple metrics, will help to reveal interactions between seemingly unrelated behaviors and serve as an early warning system for deteriorating colony health. Enhancements such as extending machine vision to automatically quantify currently qualitative measurements (e.g., brood development), implementing localized lighting to improve visibility and efficiency, and equipping the system with additional sensors (such as thermal cameras, event-based cameras, and laser scanners) will enrich the environmental and behavioral datasets collected. By integrating robotics, machine learning, and artificial intelligence, the AROBA system contributes to a paradigm shift in behavioral ecology, offering greater objectivity, scalability, and reproducibility than human observers and enabling large-scale data collection that can advance basic biological understanding and complexity science. Further information on future potential applications of our system is provided in the Supplementary Materials ("Future Potentials and Other Fields of Application of an AROBA system").

MATERIALS AND METHODS

The software architecture comprises modules communicating through a subscribe-publish Robot Operating System (ROS) framework. Each of the two AROBA system's modules runs a fiducial-based queen detection module, providing the queen's position to the actuator controller, which controls the actuator motors. The actuator controller also estimates the visibility, position, and state of the queen and shares this information with the other AROBA system's module. This can either mirror the first module's position or scan the comb. Camera images, queen positions, actuator motor data, as well as other system information are stored in data structures called "rosbags." These are regularly processed to extract their metadata and backed up to a Network Attached Storage system. The data can then be further processed by a set of analytics modules that are run on demand.

Biological aspects of the study

The western honey bee subspecies *Apis mellifera carnica* Pollmann was used in this study. The colony was maintained at the University of Graz under strict animal welfare guidelines. The colony, established in March 2023 with approximately 2000 bees, was free to forage outside the laboratory and was fed sugar solutions at the beginning of the season to promote colony growth. The queen was marked with a fiducial marker for tracking. Standard beekeeping practices were used to maintain a healthy colony, including treatment for parasites such as *Varroa destructor*. All observations were made using near-IR light to preserve natural behavior (*70*). More details on the animal care and the biology of this study are given in the Supplementary Materials ("Biological Aspects of this Study" and "Long-term Effects on Colony Health and Behavior").

Mechatronic design of the AROBA system

Our AROBA system (Fig. 1, A and B) uses a gantry mechanism to track the queen and collect data from her behavior over the long term, which demands precision, durability, and versatility. The AROBA system supports a video camera; hence, the image quality depends on the mechanisms and motion control performance. The structure, the actuation, and the control systems were individually designed considering the requirements and constraints of the vision system. Our system integration prioritized stability and adaptability to work in a vertical plane, which is necessary according to the observation hive's configuration. The main structure uses aluminum profiles allowing sufficient sturdiness while keeping the resulting structure lightweight for an operator to move it during installation or maintenance. The motion accuracy was enhanced by incorporating linear actuation systems, including feed drive ball screws and linear guides, to improve efficiency and stability.

Stepper servo motors with microstepping capability ensure accuracy in positioning, ultimately facilitating tracking the queen's motion. The system driver receives position and velocity commands and sends feedback on its current state to the management software. The main driver of the system was implemented on an ESP32 development board, which is reliable to run the system continuously. However, management software was developed to make a bridge between the ESP32 driver and the vision system for more efficient communication with other nodes and subsystems in the ROS network. The management software used the ROS communication protocol for convenient access in sending commands and receiving data for other nodes, particularly to and from the vision software. The final mechatronic system works continuously to follow the queen and scans the hive for additional data collection when the queen is resting on the other side of the hive. The integration of the AROBA system's hardware, the driver, and the vision software allows continuous data collection. The operator's supervision is needed for health monitoring and necessary maintenance only. Also, we determined how often the system needs recalibration according to the vision system's criterion for the mechanism precision. We evaluated the performance and precision of the developed mechanism through a series of experiments. In those tests, the vision system was used to measure the mechanism's repeatability and precision. The test scenario included 8 hours of repetitive sweeping motion to measure the trajectory-following accuracy and the drift after the completion of each round. According to the results obtained from a series of experiments, the mechanism had less than 10 mm of drift after traversing a 1-km distance. The AROBA mechanism was designed for observation, and it did not have any interaction with the bees inside the observation hive. Moreover, passive isolation with antivibration connectors was applied to make sure that the mechanism did not affect the experiment's conditions. More information is given in the Supplementary Materials ("Overall System Design," "Observation Hive," "Hardware of our AROBA System," and "Detailed Specifics of the Mechatronics Design").

Vision and control of our AROBA system

The system's control software is based on ROS. Thus, the software is composed of several networked modules, communicating via a standardized subscribe-publish framework. These modules process the motor data and camera images, control the movement of the

AROBA system's actuators, handle data storage, and extract data required to establish the KBMs (Fig. 1, C to E).

Each AROBA system's module used an IR camera, which provides 1920 pixel–by–1080 pixel images at 30 frames per second. More information is given in the Supplementary Materials ("Vision System of our AROBA"). For the queen and worker bee tracking, the software set the camera zoom to provide images with 15 pixels per millimeter, and the focus was optimized for sharp pictures of the bees. Detailed comb scans were captured with the camera lens focus and zoom set to provide sharp images of the comb at 40 pixels per millimeter. The images could be composed using odometry-based stitching as in Figs. 2 (A and E), 3A, and 4A and in movie S1. The images were also analyzed by a fiducial marker detection and a 6-degree-of-freedom (DoF) localization method, WhyCode (*71*). The honey bee queen was equipped with a circular fiducial marker attached to the dorsal side of her thorax. Although the pattern drawn on the marker was not standard, its size (2.1 mm), shape (circle), and material (Xerox NeverTear with Belton acrylic varnish) were similar to the markers commonly used by beekeepers to identify the queen quickly.

Both the AROBA system's left and right actuators were controlled independently. However, they informed each other about the queen's visibility, position, and speed to coordinate their activity and movement. The strategy of this cooperation is described briefly in the Introduction section, depicted schematically in Fig. 1, and described in more detail in the Supplementary Materials ("Queen Detection and Tracking" and "High-Level Control, Self-Diagnostics, Power and Data Management"). A dedicated computer performed diagnostics, data, and power management routines. System modules that exhibited a drop in the expected outgoing data stream were considered faulty and were restarted in software. In case the faulty behavior persisted after three software restarts, a hardware restart was performed through power management. More details on the data flow are given in the Supplementary Materials ("Software Integration and Data Flow").

Vision-based detection, localization, tracking, and classification

Establishing the KBMs relies on computer vision methods that track the queen, detect the egg laying (oviposition), and localize the worker bees. More details on the method integration are in the Supplementary Materials ("Software Integration and Data Flow"). Tracking the queen was achieved by the WhyCode (*71*) method, which was capable of reliable detection and precise 6-DoF localization of a marker attached to the queen's thorax. To determine the method's detection performance, we annotated 16,230 images from 1 day and both sides of the hive at approximately 10-s intervals. The established precision and recall were 1.00 and 0.952, respectively. The 6414 images that contained the queen were used to determine the average and maximal localization errors, which were 0.847 and 2.23 pixels, corresponding to 56.7 and 149 μm.

Oviposition event candidates were detected through analysis of the queen's motion patterns provided by her tracking. Image series captured ±10 s around these events were forwarded to a two-dimensional CNN that classifies whether an oviposition event occurred in the single forwarded frames. These single-frame classifications were then stored in a classification vector from which we calculated whether an oviposition event occurred in the image series and when, within this image series, the oviposition occurred. The resulting daily dataset was then finally forwarded to a post hoc filtering algorithm that removes spatially isolated oviposition events as well as impossible oviposition events on the wooden frame of the comb.

Candidate events extracted from the observation data of 28 July were used for training the CNN. This resulted in 31,964 annotated images with a 400 pixel–by–400 pixel resolution, which were split up into 70% training data, 15% validation data, and 15% testing data. For real-world performance evaluation, independent testing data (in the form of candidate events extracted on the 10th of October) were used. This resulted in an overall performance of the pipeline of a precision of 0.9338, a recall of 0.9513, an accuracy of 0.9338, and an F1 score of 0.9425 {more information is given in the Supplementary Materials ["Measuring the Oviposition Rate (Egg-Laying Rate) of the Queen"]}. This algorithmic pipeline was used to analyze a 30-day-long dataset from 20 September to 19 October.

The worker bee localization was achieved by BeeYOLOv8, a YOLOv8 (*72*) network that was fine-tuned to detect worker bees using comb images obtained from the AROBA system. The orientations of the bees are estimated with a CNN-based model. More details are given in the Supplementary Materials (fig. S2 and "Worker Bee Detection"). The model uses the bee images produced by the object detector as input. It outputs the sine and cosine of the angle of the bees. When used for court bee detection, the method achieves precision, recall, and F1 score values of 0.82, 0.84, and 0.83, respectively. The worker bee population estimation must include more crowded and cluttered areas of the comb, where the method achieves 0.887 precision, 0.470 recall, and an F1 score of 0.62. More details are described in the Supplementary Materials ("Worker Bee Detection," "Court Bee Detection," and "Establishing the Key Behavioral Metrics").

Supplementary Materials

The PDF file includes:

Extended Materials and Methods
Tables S1 to S5
Figs. S1 to S17
Extended Discussion
Legends for movies S1 to S10
References (*73–111*)

Other Supplementary Material for this manuscript includes the following:

Movies S1 to S10

REFERENCES AND NOTES

1. K. H. Erb, T. Kastner, C. Plutzar, A. L. S. Bais, N. Carvalhais, T. Fetzel, S. Gingrich, H. Haberl, C. Lauk, M. Niedertscheider, J. Pongratz, M. Thurner, S. Luyssaert, Unexpectedly large impact of forest management and grazing on global vegetation biomass. *Nature* **553**, 73–76 (2018).
2. V. Christensen, M. Coll, C. Piroddi, J. Steenbeek, J. Buszowski, D. Pauly, A century of fish biomass decline in the ocean. *Mar. Ecol. Prog. Ser.* **512**, 155–166 (2014).
3. J. E. Watson, D. F. Shanahan, M. Di Marco, J. Allan, W. F. Laurance, E. W. Sanderson, B. Mackey, O. Venter, Catastrophic declines in wilderness areas undermine global environment targets. *Curr. Biol.* **26**, 2929–2934 (2016).
4. C. A. Hallmann, M. Sorg, E. Jongejans, H. Siepel, N. Hofland, H. Schwan, W. Stenmans, A. Müller, H. Sumser, T. Hörren, D. Goulson, H. De Kroon, More than 75 percent decline over 27 years in total flying insect biomass in protected areas. *PLOS ONE* **12**, e0185809 (2017).
5. R. M. Dalton, N. C. Underwood, D. W. Inouye, M. E. Soulé, B. D. Inouye, Long-term declines in insect abundance and biomass in a subalpine habitat. *Ecosphere* **14**, e4620 (2023).
6. G. D. Powney, C. Carvell, M. Edwards, R. K. Morris, H. E. Roy, B. A. Woodcock, N. J. Isaac, Widespread losses of pollinating insects in Britain. *Nat. Commun.* **10**, 1–6 (2019).
7. K. R. Shivanna, R. Tandon, M. Koul, 'Global pollinator crisis' and its impact on crop productivity and sustenance of plant diversity, in *Reproductive Ecology of Flowering Plants: Patterns and Processes*, R. Tandon, K. R. Shivanna, M. Koul, Eds. (Springer, 2020), pp. 395–413.

8. P. G. Kevan, P. P. Truman, The economic impacts of pollinator declines: An approach to assessing the consequences. *Conserv. Ecol.* **5**, 1–14 (2001).
9. R. G. Porto, R. F. de Almeida, O. Cruz-Neto, M. Tabarelli, B. F. Viana, C. A. Peres, A. V. Lopes, Pollination ecosystem services: A comprehensive review of economic values, research funding and policy actions. *Food Secur.* **12**, 1425–1442 (2020).
10. A. M. Klein, B. E. Vaissière, J. H. Cane, I. Steffan-Dewenter, S. A. Cunningham, C. Kremen, T. Tscharntke, Importance of pollinators in changing landscapes for world crops. *Proc. R. Soc. B* **274**, 303–313 (2007).
11. Y. P. Paudel, R. Mackereth, R. Hanley, W. Qin, Honey bees (*Apis mellifera* L.) and pollination issues: Current status, impacts, and potential drivers of decline. *J. Agric. Sci.* **7**, 93 (2015).
12. R. C. Eberhart, Y. Shi, J. Kennedy, *Swarm Intelligence* (Academic Press, 2001).
13. T. Schmickl, M. Szopek, F. Mondada, R. Mills, M. Stefanec, D. N. Hofstadler, D. Lazic, R. Barmak, F. Bonnet, P. Zahadat, Social integrating robots suggest mitigation strategies for ecosystem decay. *Front. Bioeng. Biotechnol.* **9**, 612605 (2021).
14. J. R. Harbo, Effect of population size on brood production, worker survival and honey gain in colonies of honeybees. *J. Apic. Res.* **25**, 22–29 (1986).
15. Y. Le Conte, G. Arnold, P. H. Desenfant, Influence of brood temperature and hygrometry variations on the development of the honey bee ectoparasite *Varroa jacobsoni* (Mesostigmata: Varroidae). *Environ. Entomol.* **19**, 1780–1785 (1990).
16. S. Camazine, Self-organizing pattern formation on the combs of honey bee colonies. *Behav. Ecol. Sociobiol.* **28**, 61–76 (1991).
17. J. Rangel, J. J. Keller, D. R. Tarpy, The effects of honey bee (*Apis mellifera* L.) queen reproductive potential on colony growth. *Insectes Soc.* **60**, 65–73 (2013).
18. T. Pankiw, M. L. Winston, K. N. Slessor, Queen attendance behavior of worker honey bees (*Apis mellifera* L.) that are high and low responding to queen mandibular pheromone. *Insectes Soc.* **42**, 371–378 (1995).
19. M. D. Allen, The honeybee queen and her attendants. *Anim. Behav.* **8**, 201–208 (1960).
20. F. Huber, *Observations on the Natural History of Bees* (Longman, Hurst, Rees, and Orme, 1806).
21. K. Von Frisch, *Tanzsprache und Orientierung der Bienen* (Springer-Verlag, 1965).
22. N. N. Tinbergen, *The Study of Instinct* (Clarendon Press, 1954).
23. K. Z. Lorenz, *The Comparative Method in Studying Innate Behavior Patterns* (Routledge, 1963).
24. P. Marler, D. R. Griffin, The 1973 Nobel Prize for physiology or medicine. *Science* **182**, 464–466 (1973).
25. M. Szopek, T. Schmickl, R. Thenius, G. Radspieler, K. Crailsheim, Dynamics of collective decision making of honeybees in complex temperature fields. *PLOS ONE* **8**, e76250 (2013).
26. R. Scheiner, C. I. Abramson, R. Brodschneider, K. Crailsheim, W. M. Farina, S. Fuchs, B. Grünewald, S. Hahshold, M. Karrer, G. Koeniger, N. Koeniger, R. Menzel, S. Mujagic, G. Radspieler, T. Schmickl, C. Schneider, A. J. Siegel, M. Szopek, R. Thenius, Standard methods for behavioural studies of *Apis mellifera*. *J. Apic. Res.* **52**, 1–58 (2013).
27. K. Žampachů, J. Ulrich, T. Rouček, M. Stefanec, D. Dvořáček, L. Fedotoff, D. N. Hofstadler, F. Rekabi-Bana, G. Broughton, F. Arvin, T. Schmickl, T. Krajník, A vision-based system for social insect tracking, in *Proceedings of the 2022 2nd IEEE International Conference on Robotics, Automation and Artificial Intelligence* (IEEE, 2022), pp. 277–283.
28. F. Wario, B. Wild, R. Rojas, T. Landgraf, Automatic detection and decoding of honey bee waggle dances. *PLOS ONE* **12**, e0188626 (2017).
29. K. Bozek, L. Hebert, Y. Portugal, A. S. Mikheyev, G. J. Stephens, Markerless tracking of an entire honey bee colony. *Nat. Commun.* **12**, 1733 (2021).
30. M. Stefanec, H. Oberreiter, M. A. Becher, G. Haase, T. Schmickl, Effects of sinusoidal vibrations on the motion response of honeybees. *Front. Phys.* **9**, 670555 (2021).
31. A. Feldman, T. Balch, Representing honey bee behavior for recognition using human trainable models. *Adapt. Behav.* **12**, 241–250 (2004).
32. T. Gernat, T. Jagla, B. M. Jones, M. Middendorf, G. E. Robinson, Automated monitoring of honey bees with barcodes and artificial intelligence reveals two distinct social networks from a single affiliative behavior. *Sci. Rep.* **13**, 1541 (2023).
33. T. N. Ngo, D. J. A. Rustia, E. C. Yang, T. T. Lin, Automated monitoring and analyses of honey bee pollen foraging behavior using a deep learning-based imaging system. *Comput. Electron. Agric.* **187**, 106239 (2021).
34. T. P. Kucner, M. Magnusson, S. Mghames, L. Palmieri, F. Verdoja, C. S. Swaminathan, T. Krajník, E. Schaffernicht, N. Bellotto, M. Hanheide, A. J. Lilienthal, Survey of maps of dynamics for mobile robots. *Int. J. Robot. Res.* **42**, 977–1006 (2023).
35. J. M. Santos, T. Krajník, J. P. Fentanes, T. Duckett, Lifelong information-driven exploration to complete and refine 4-D spatio-temporal maps. *IEEE Robot. Autom. Lett.* **1**, 684–691 (2016).
36. S. Molina, G. Cielniak, T. Duckett, Robotic exploration for learning human motion patterns. *IEEE Trans. Robot.* **38**, 1304–1318 (2021).
37. X. Xu, W. Yang, B. Tian, X. Sui, W. Chi, Y. Rao, C. Tang, Quantitative investigation reveals distinct phases in *Drosophila* sleep. *Commun. Biol.* **4**, 364 (2021).
38. J. Watmough, A general model of pheromone transmission within honey bee hives. *J. Theor. Biol.* **189**, 159–170 (1997).
39. K. Naumann, M. L. Winston, K. N. Slessor, G. D. Prestwich, B. Latli, Intra-nest transmission of aromatic honey bee queen mandibular gland pheromone components: Movement as a unit. *Can. Entomol.* **124**, 917–934 (1992).
40. D. R. Yoerger, A. F. Govindarajan, J. C. Howland, J. K. Llopiz, P. H. Wiebe, M. Curran, J. Fujii, D. Gomez-Ibanez, K. Katija, B. H. Robinson, B. W. Hobson, M. Risi, S. M. Rock, A hybrid underwater robot for multidisciplinary investigation of the ocean twilight zone. *Sci. Robot.* **6**, eabe1901 (2021).
41. G. Li, T. W. Wong, B. Shih, C. Guo, L. Wang, J. Liu, J. Yan, B. Wu, F. Yu, Y. Chen, Y. Liang, Y. Xue, C. Wang, S. He, L. Wen, M. T. Tolley, A. Zhang, C. Laschi, T. Li, Bioinspired soft robots for deep-sea exploration. *Nat. Commun.* **14**, 7097 (2023).
42. R. K. Katzschmann, J. DelPreto, R. MacCurdy, D. Rus, Exploration of underwater life with an acoustically controlled soft robotic fish. *Sci. Robot.* **3**, eaar3449 (2018).
43. J. C. Hodgson, R. Mott, S. M. Baylis, T. T. Pham, S. Wotherspoon, A. D. Kilpatrick, R. R. Segaran, I. Reid, A. Terauds, L. P. Koh, Drones count wildlife more accurately and precisely than humans. *Methods Ecol. Evol.* **9**, 1160–1167 (2018).
44. J. T. Beaver, R. W. Baldwin, M. Messinger, C. H. Newbolt, S. S. Ditchkoff, M. R. Silman, Evaluating the use of drones equipped with thermal sensors as an effective method for estimating wildlife. *Wildl. Soc. Bull.* **44**, 434–443 (2020).
45. A. Ilgün, K. Angelov, M. Stefanec, S. Schönwetter-Fuchs, V. Stokanic, J. Vollmann, D. N. Hofstadler, M. H. Kärcher, H. Mellmann, V. Taliaronak, A. Kviesis, V. Komasilovs, M. A. Becher, M. Szopek, D. M. Dormagen, R. Barmak, E. Bairaktarov, M. Broisin, R. Thenius, R. Mills, S. C. Nicolis, A. Campo, A. Zacepins, S. Petrov, J. L. Deneubourg, F. Mondada, T. Landgraf, V. V. Hafner, T. Schmickl, Bio-hybrid systems for ecosystem level effects, in *Proceedings of the ALIFE 2021: The 2021 Conference on Artificial Life* (MIT Press, 2021).
46. F. E. Murphy, M. Magno, P. Whelan, E. P. Vici, b+ WSN: Smart beehive for agriculture, environmental, and honey bee health monitoring—Preliminary results and analysis, in *2015 IEEE Sensors Applications Symposium (SAS)* (IEEE, 2015).
47. W. G. Meikle, N. Holst, Application of continuous monitoring of honeybee colonies. *Apidologie* **46**, 10–22 (2015).
48. A. Zacepins, A. Kviesis, V. Komasilovs, F. R. Muhammad, Monitoring system for remote bee colony state detection. *Balt. J. Modern Comp.* **8**, 461–470 (2020).
49. T. D. Seely, Queen substance dispersal by messenger workers in honeybee colonies. *Behav. Ecol. Sociobiol.* **5**, 391–415 (1979).
50. T. Ohtani, Behaviors of adult queen honeybees within observation hives. I. Behavioral patterns. *Hum. Nat.* **3**, 37–77 (1994).
51. M. D. Allen, Observations on honeybees attending their queen. *Brit. J. Anim. Behav.* **3**, 66–69 (1955).
52. T. Schmickl, B. Blaschon, B. Gurmann, K. Crailsheim, Collective and individual nursing investment in the queen and in young and old honeybee larvae during foraging and non-foraging periods. *Insectes Soc.* **50**, 174–184 (2003).
53. B. M. Jones, V. D. Rao, T. Gernat, T. Jagla, A. C. Cash-Ahmed, B. E. R. Rubin, T. J. Comi, S. Bhogale, S. S. Husain, C. Blatti, M. Middendorf, S. Sinha, S. Chandrasekaran, G. E. Robinson, Individual differences in honey bee behavior enabled by plasticity in brain gene regulatory networks. *eLife* **9**, e62850 (2020).
54. T. Gernat, V. D. Rao, M. Middendorf, H. Dankowicz, N. Goldenfeld, G. E. Robinson, Automated monitoring of behavior reveals bursty interaction patterns and rapid spreading dynamics in honeybee social networks. *Proc. Natl. Acad. Sci. U.S.A.* **115**, 1433–1438 (2018).
55. F. Boenisch, B. Rosemann, B. Wild, D. Dormagen, F. Wario, T. Landgraf, Tracking all members of a honey bee colony over their lifetime using learned models of correspondence. *Front. Robot. AI* **5**, 35 (2018).
56. B. Wild, D. M. Dormagen, A. Zachariae, M. L. Smith, K. S. Traynor, D. Brockmann, I. D. Couzin, T. Landgraf, Social networks predict the life and death of honey bees. *Nat. Commun.* **12**, 1110 (2021).
57. T. Kimura, M. Ohashi, R. Okada, H. Ikeno, A new approach for the simultaneous tracking of multiple honeybees for analysis of hive behavior. *Apidologie* **42**, 607–617 (2011).
58. K. Bozek, L. Hebert, A. S. Mikheyev, G. J. Stephens, Towards dense object tracking in a 2D honeybee hive, in *Proceedings of the IEEE Conference on Computer Vision and Pattern Recognition* (IEEE, 2018), pp. 4185–4193.
59. P. Kongsilp, U. Taetragool, O. Duangphakdee, Individual honey bee tracking in a beehive environment using deep learning and Kalman filter. *Sci. Rep.* **14**, 1061 (2024).
60. C. Tsai, T. Ngo, E. Yang, T. Lin, Image processing algorithms of tracking and movement pattern analysis for honeybees in a beehive, paper presented at the CIGR-AgEng Conference, Aarhus, Denmark, 26 to 29 June 2016.
61. P. Siefert, R. Hota, V. Ramesh, B. Grünewald, Chronic within-hive video recordings detect altered nursing behaviour and retarded larval development of neonicotinoid treated honey bees. *Sci. Rep.* **10**, 8727 (2020).
62. T. Landgraf, R. Rojas, H. Nguyen, F. Kriegel, K. Stettin, Analysis of the waggle dance motion of honeybees for the design of a biomimetic honeybee robot. *PLOS ONE* **6**, e21354 (2011).

63. D. M. Dormagen, B. Wild, F. Wario, T. Landgraf, Machine learning reveals the waggle drift's role in the honey bee dance communication system. *PNAS Nexus* **2**, pgad275 (2023).
64. G. Chiron, P. Gomez-Krämer, M. Ménard, Detecting and tracking honeybees in 3D at the beehive entrance using stereo vision. *EURASIP J. Image Video Process.* **59**, 1–17 (2013).
65. C. Yang, J. Collins, Improvement of honey bee tracking on 2D video with Hough transform and Kalman filter. *J. Signal Process. Syst.* **90**, 1639–1650 (2018).
66. C. Sun, P. Gaydecki, A visual tracking system for honey bee (Hymenoptera: Apidae) 3D flight trajectory reconstruction and analysis. *J. Insect Sci.* **21**, 17 (2021).
67. H. Ai, S. Takahashi, The lifelog monitoring system for honeybees: RFID and camera recordings in an observation hive. *J. Robot. Mechatron.* **33**, 457–465 (2021).
68. P. Tenczar, C. C. Lutz, V. D. Rao, N. Goldenfeld, G. E. Robinson, Automated monitoring reveals extreme interindividual variation and plasticity in honeybee foraging activity levels. *Anim. Behav.* **95**, 41–48 (2014).
69. P. Nunes-Silva, M. Hrncir, J. T. F. Guimarães, H. Arruda, L. Costa, G. Pessin, J. O. Siqueira, P. de Souza, V. L. Imperatriz-Fonseca, Applications of RFID technology on the study of bees. *Insectes Soc.* **66**, 15–24 (2019).
70. D. Peitsch, A. Fietz, H. Hertel, J. de Souza, D. F. Ventura, R. Menzel, The spectral input systems of hymenopteran insects and their receptor-based colour vision. *J. Comp. Physiol. A* **170**, 23–40 (1992).
71. J. Ulrich, J. Blaha, A. Alsayed, T. Rouček, F. Arvin, T. Krajník, Real time fiducial marker localisation system with full 6 DOF pose estimation. *SIGAPP Appl. Comput. Rev.* **23**, 20–35 (2023).
72. G. Jocher, A. Chaurasia, J. Qiu, Ultralytics YOLO (version 8.0.0), 2023; https://github.com/ultralytics/ultralytics.
73. M. Beekman, F. L. W. Ratnieks, Long-range foraging by the honey-bee, *Apis mellifera* L. *Funct. Ecol.* **14**, 490–496 (2000).
74. R. M. Goodwin, H. M. Cox, M. A. Taylor, L. J. Evans, H. M. McBrydie, Number of honey bee visits required to fully pollinate white clover (*Trifolium repens*) seed crops in Canterbury, New Zealand. *New Zeal. J. Crop Hortic. Sci.* **39**, 7–19 (2011).
75. J. H. Fewell, M. L. Winston, Colony state and regulation of pollen foraging in the honey bee, *Apis mellifera* L. *Behav. Ecol. Sociobiol.* **30**, 387–393 (1992).
76. S. A. Khalifa, E. H. Elshafiey, A. A. Shetaia, A. A. Abd El-Wahed, A. F. Algethami, S. G. Musharraf, M. F. AlAjmi, C. Zhao, S. H. D. Masry, M. M. Abdel-Daim, M. F. Halabi, G. Kai, Y. Al Naggar, M. Bishr, M. A. M. Diab, H. R. El-Seedi, Overview of bee pollination and its economic value for crop production. *Insects* **12**, 688 (2021).
77. B. J. Phiri, D. Fèvre, A. Hidano, Uptrend in global managed honey bee colonies and production based on a six-decade viewpoint. *Sci. Rep.* **12**, 21298 (2022).
78. Fortune Business Insights, "Honey market size, share & COVID-19 impact analysis, by type (alfalfa, buckwheat, wildflower, clover, acacia, and others), by application (food & beverages, personal care & cosmetics, pharmaceuticals, and others), by packaging (glass jar, bottle, tub, tube, and others), and regional forecast, 2022–2029," Report ID FBI100551 (2024); https://www.fortunebusinessinsights.com/industry-reports/honey-market-100551.
79. J. R. Reilly, D. R. Artz, D. Biddinger, K. Bobiwash, N. K. Boyle, C. Brittain, J. Brokaw, J. W. Campbell, J. Daniels, E. Elle, J. D. Ellis, S. J. Fleischer, J. Gibbs, R. L. Gillespie, K. B. Gundersen, L. Gut, G. Hoffman, N. Joshi, O. Lundin, K. Mason, C. M. McGrady, S. S. Peterson, T. L. Pitts-Singer, S. Rao, N. Rothwell, L. Rowe, K. L. Ward, N. M. Williams, J. K. Wilson, R. Isaacs, R. Winfree, Crop production in the USA is frequently limited by a lack of pollinators. *Proc. Roy. Soc. B* **287**, 20200922 (2020).
80. R. E. Snodgrass, *Anatomy of the Honey Bee* (Cornell Univ. Press, 1956).
81. L. Bortolotti, C. Costa, Chemical communication in the honey bee society, in *Neurobiology of Chemical Communication*, C. Mucignat-Caretta, Ed. (CRC Press/Taylor & Francis, 2014), chap. 5.
82. J. Halloy, G. Sempo, G. Caprari, C. Rivault, M. Asadpour, F. Tâche, I. Saïd, V. Durier, S. Canonge, J. M. Amé, C. Detrain, N. Correll, A. Martinoli, F. Mondada, R. Siegwart, J. L. Deneubourg, Social integration of robots into groups of cockroaches to control self-organized choices. *Science* **318**, 1155–1158 (2007).
83. F. Bonnet, L. Cazenille, A. Séguret, A. Gribovskiy, B. Collignon, J. Halloy, F. Mondada, Design of a modular robotic system that mimics small fish locomotion and body movements for ethological studies. *Int. J. Adv. Rob. Syst.* **14**, 1729881417706628 (2017).
84. F. Bonnet, A. Gribovskiy, J. Halloy, F. Mondada, Closed-loop interactions between a shoal of zebrafish and a group of robotic fish in a circular corridor. *Swarm Intell.* **12**, 227–244 (2018).
85. D. Bierbach, T. Landgraf, P. Romanczuk, J. Lukas, H. Nguyen, M. Wolf, J. Krause, Using a robotic fish to investigate individual differences in social responsiveness in the guppy. *R. Soc. Open Sci.* **5**, 181026 (2018).
86. A. Gribovskiy, J. Halloy, J. L. Deneubourg, H. Bleuler, F. Mondada, Towards mixed societies of chickens and robots, in *2010 IEEE/RSJ International Conference on Intelligent Robots and Systems* (IEEE, 2010), pp. 4722–4728.
87. Q. Shi, H. Ishii, K. Tanaka, Y. Sugahara, A. Takanishi, S. Okabayashi, Q. Huang, T. Fukuda, Behavior modulation of rats to a robotic rat in multi-rat interaction. *Bioinspir. Biomim.* **10**, 056011 (2015).
88. P. K. Sahoo, D. K. Kushwaha, N. C. Pradhan, Y. Makwana, M. Kumar, M. Jatoliya, M. A. Naik, I. Mani, Robotics application in agriculture, paper presented at the 55th Annual Convention of Indian Society of Agricultural Engineers and International, Pusa, India, 23 to 25 November 2021.
89. P. Phamduy, G. Polverino, R. C. Fuller, M. Porfiri, Fish and robot dancing together: Bluefin killifish females respond differently to the courtship of a robot with varying color morphs. *Bioinspir. Biomim.* **9**, 036021 (2014).
90. D. Romano, G. Benelli, E. Donati, D. Remorini, A. Canale, C. Stefanini, Multiple cues produced by a robotic fish modulate aggressive behaviour in Siamese fighting fishes. *Sci. Rep.* **7**, 4667 (2017).
91. D. Romano, C. Stefanini, Unveiling social distancing mechanisms via a fish-robot hybrid interaction. *Biol. Cybern.* **115**, 565–573 (2021).
92. A. A. Brown, M. F. Brown, S. R. Folk, B. A. Utter, Archerfish respond to a hunting robotic conspecific. *Biol. Cybern.* **115**, 585–598 (2021).
93. S. Marras, M. Porfiri, Fish and robots swimming together: Attraction towards the robot demands biomimetic locomotion. *J. R. Soc. Interface* **9**, 1856–1868 (2012).
94. G. Polverino, N. Abaid, V. Kopman, S. Macrì, M. Porfiri, Zebrafish response to robotic fish: Preference experiments on isolated individuals and small shoals. *Bioinspir. Biomim.* **7**, 036019 (2012).
95. G. Polverino, M. Porfiri, Mosquitofish (*Gambusia affinis*) responds differentially to a robotic fish of varying swimming depth and aspect ratio. *Behav. Brain Res.* **250**, 133–138 (2013).
96. M. Kruusmaa, G. Rieucau, J. C. C. Montoya, R. Markna, N. O. Handegard, Collective responses of a large mackerel school depend on the size and speed of a robotic fish but not on tail motion. *Bioinspir. Biomim.* **11**, 056020 (2016).
97. S. Butail, G. Polverino, P. Phamduy, F. Del Sette, M. Porfiri, Fish-robot interactions in a free-swimming environment: effects of speed and configuration of robots on live fish, in *Proc. SPIE 9055, Bioinspiration, Biomimetics, and Bioreplication* (SPIE, 2014).
98. M. Kruusmaa, R. Gkliva, J. A. Tuhtan, A. Tuvikene, J. A. Alfredsen, Salmon behavioural response to robots in an aquaculture sea cage. *R. Soc. Open Sci.* **7**, 191220 (2020).
99. D. Romano, G. Benelli, C. Stefanini, Opposite valence social information provided by bio-robotic demonstrators shapes selection processes in the green bottle fly. *J. R. Soc. Interface* **18**, 20210056 (2021).
100. D. Romano, G. Benelli, C. Stefanini, How aggressive interactions with biomimetic agents optimize reproductive performances in mass-reared males of the Mediterranean fruit fly. *Biol. Cybern.* **117**, 249–258 (2023).
101. D. Romano, G. Benelli, C. Stefanini, Escape and surveillance asymmetries in locusts exposed to a Guinea fowl-mimicking robot predator. *Sci. Rep.* **7**, 12825 (2017).
102. A. Michelsen, B. B. Andersen, W. H. Kirchner, M. Lindauer, Honeybees can be recruited by a mechanical model of a dancing bee. *Naturwissenschaften* **76**, 277–280 (1989).
103. W. H. Kirchner, W. F. Towne, The sensory basis of the honeybee's dance language. *Sci. Am.* **270**, 74–80 (1994).
104. T. Landgraf, M. Oertel, D. Rhiel, R. Rojas, A biomimetic honeybee robot for the analysis of the honeybee dance communication system, in *2010 IEEE/RSJ International Conference on Intelligent Robots and Systems* (IEEE, 2010), pp. 3097–3102.
105. T. Landgraf, M. Oertel, A. Kirbach, R. Menzel, R. Rojas, Imitation of the honeybee dance communication system by means of a biomimetic robot, in *Biomimetic and Biohybrid Systems: First International Conference, Living Machines 2012, Barcelona, Spain, July 9–12, 2012, Proceedings*, T. J. Prescott, N. F. Lepora, A. Mura, P. F. M. J. Verschure, Eds., vol. 7375 of *Lecture Notes in Computer Science* (Springer, 2012), pp. 132–143.
106. F. Bonnet, R. Mills, M. Szopek, S. Schönwetter-Fuchs, J. Halloy, S. Bogdan, L. Correia, F. Mondada, T. Schmickl, Robots mediating interactions between animals for interspecies collective behaviors. *Sci. Robot.* **4**, eaau7897 (2019).
107. K. Griparić, T. Haus, D. Miklić, M. Polić, S. Bogdan, A robotic system for researching social integration in honeybees. *PLOS ONE* **12**, e0181977 (2017).
108. P. Mariano, Z. Salem, R. Mills, S. Schönwetter-Fuchs-Schistek, L. Correia, T. Schmickl, Evolving robot controllers for a bio-hybrid system, in *Proceedings of the ALIFE 2018: The 2018 Conference on Artificial Life* (MIT Press, 2018), pp. 155–162.
109. R. Barmak, M. Stefanec, D. N. Hofstadler, L. Piotet, S. Schönwetter-Fuchs-Schistek, F. Mondada, T. Schmickl, R. Mills, A robotic honeycomb for interaction with a honeybee colony. *Sci. Robot.* **8**, eadd7385 (2023).
110. R. Barmak, D. N. Hofstadler, M. Stefanec, L. Piotet, R. Cherfan, T. Schmickl, F. Mondada, R. Mills, Biohybrid superorganisms—On the design of a robotic system for thermal interactions with honeybee colonies. *IEEE Access* **12**, 50849–50871 (2024).
111. M. Stefanec, D. N. Hofstadler, T. Krajník, A. E. Turgut, H. Alemdar, B. Lennox, E. Şahin, F. Arvin, T. Schmickl, A minimally invasive approach towards "ecosystem hacking" with honeybees. *Front. Robot. AI* **9**, 791921 (2022).

Acknowledgments: We thank H. Pascher for support in constructing the experimental setup, P. Delanoy for system maintenance, J. Vollmann for dedicated honey bee care, G. Broughton for expertise in network technologies, D. Dvoracek for assistance in forensic analysis, and D. Tintěra for consultation on queen markers. We also thank I. Grassl for proofreading and suggesting improvements to the manuscript. **Funding:** This article is supported by the EU grant RoboRoyale (grant no. 964492). T.S., M.St., D.N.H., and L.A.F. are supported by the Field of Excellence COLIBRI (Complexity of Life in Basic Research and Innovation) of the University of Graz. T.K. and T.R. are supported by the MEYS (Ministry of Education, Youth and Sports) project ROBOPROX no.

CZ.02.01.01/00/22_008/0004590 co-funded by the EU. **Author contributions:** Conceptualization: T.S., T.K., F.A., E.Ş., J.U., M.St., and F.R.-B. Methodology: F.R.-B., T.K., M.Sa., J.U., F.A., M.St., J.B., L.A.F., J.J., T.R., E.Ş., T.S., H.A., B.Y.G., D.N.H., E.E.K., and A.E.T. Software: J.U., T.K., L.A.F., F.R.-B., T.R., M.St., D.N.H., K.Ž., M.Sa., J.J., H.A., B.Y.G., E.E.K., and T.S. Validation: L.A.F., J.U., J.B., and T.K. Formal analysis: J.B., T.K., J.U., T.S., and L.A.F. Investigation: M.St., T.K., F.R.-B., J.U., L.A.F., D.N.H., T.S., J.B., J.J., T.R., and B.Y.G. Resources: T.S., F.A., T.K., E.Ş., H.A., and A.E.T. Data curation: J.U., L.A.F., D.N.H., T.K., J.J., T.R., J.B., K.Ž., B.E., M.St., E.Ş., and H.A. Writing—original draft: T.S., T.K., M.St., L.A.F., F.R.-B., J.U., J.B., J.J., E.Ş., H.A., A.E.T., and F.A. Writing—review and editing: T.S., T.K., F.A., M.St., F.R.-B., E.Ş., A.E.T., J.U., J.B., D.N.H., H.A., L.A.F., B.E., T.R., B.Y.G., and M.Sa. Visualization: T.K., M.St., T.S., J.U., F.A., F.R.-B., J.B., L.A.F., B.Y.G., and M.Sa. Supervision: T.K., T.S., F.A., H.A., and A.E.T. Project administration: F.A., T.K., T.S., and E.Ş. Funding acquisition: F.A., T.S., T.K., and E.Ş. **Competing interests:** The authors declare that they have no competing interests. **Data and materials availability:** Supplementary data and code supporting the findings of this study are publicly available on Zenodo at the following links: supplementary data, https://zenodo.org/records/13801588; supplementary code, https://zenodo.org/records/13801588.

Submitted 22 December 2023
Accepted 23 September 2024
Published 16 October 2024
10.1126/scirobotics.adn6848